Science Advances
AAAS

advances.sciencemag.org/cgi/content/full/5/8/eaax0064/DC1

Supplementary Materials for

A prokaryotic-eukaryotic hybrid viral vector for delivery of large cargos of genes and proteins into human cells

Jingen Zhu, Pan Tao, Marthandan Mahalingam, Jian Sha, Paul Kilgore, Ashok K. Chopra, Venigalla Rao*

*Corresponding author. Email: rao@cua.edu

Published 21 August 2019, *Sci. Adv.* **5**, eaax0064 (2019)
DOI: 10.1126/sciadv.aax0064

This PDF file includes:

SUPPLEMENTARY MATERIALS

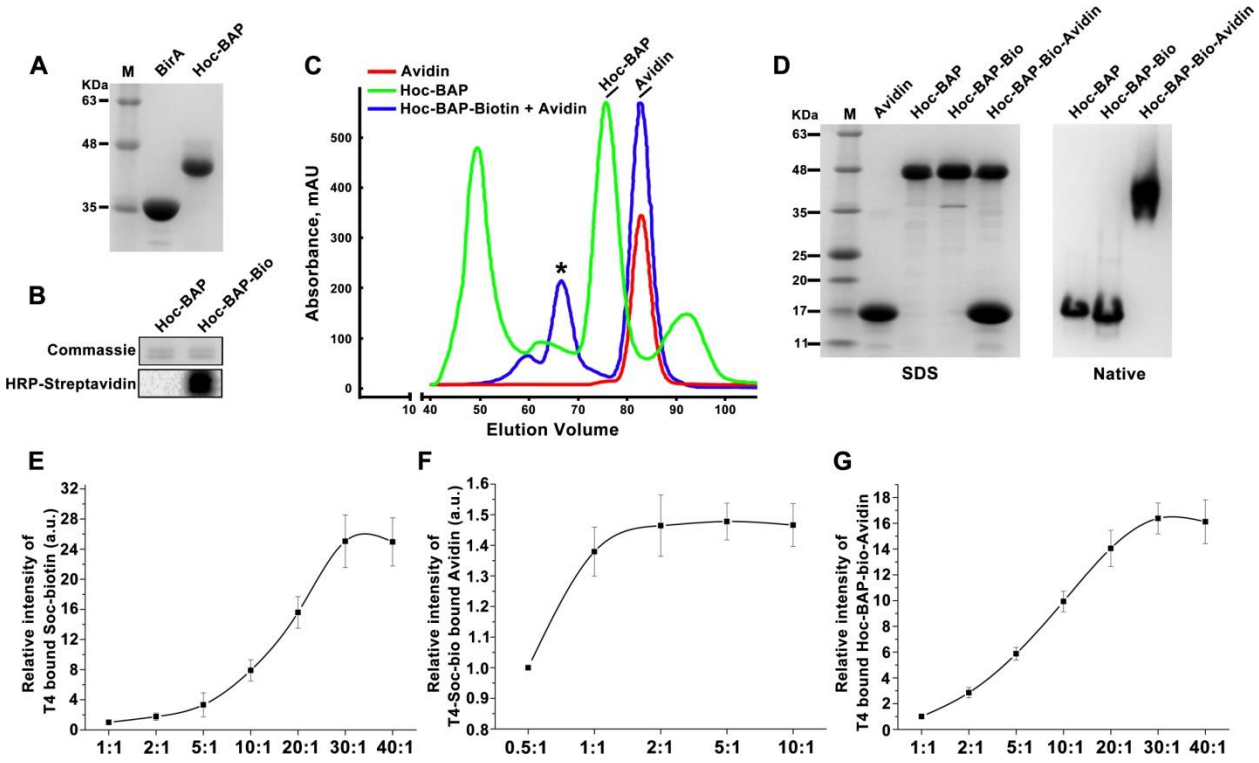

Fig. S1. Characterization of HBBA and quantification of the SBA and HBBA displays. (A) Examination of recombinant BirA and Hoc-BAP by SDS-PAGE. **(B)** Coomassie staining and HRP-streptavidin western blot for Hoc-BAP and Hoc-BAP-biotin. **(C)** SEC analysis of avidin, Hoc-BAP, and HBBA. The asterisk indicates the HBBA elution peak. **(D)** SDS-PAGE and native (non-denaturing)-PAGE analyses of avidin, Hoc-BAP, Hoc-BAP-biotin, and HBBA. **(E)** Soc-biotin binding curve. The density volumes of T4-bound Soc-biotin were quantified by laser densitometry based on the SDS-PAGE results shown in Fig. 3D. The intensity of T4-bound Soc-biotin at the 1:1 ratio was normalized to 1. **(F)** Statistical analysis of T4-Soc-biotin-bound avidin based on the SDS-PAGE results shown in Fig. 3E. The intensity of T4-Soc-biotin-bound avidin at the 0.5:1 ratio was normalized to 1. **(G)** Binding intensity curve of HBBA based on the SDS-PAGE results shown in Fig. 3F. The intensity of T4-bound HBBA at the 1:1 ratio was normalized to 1. The values represent the mean ± SD.

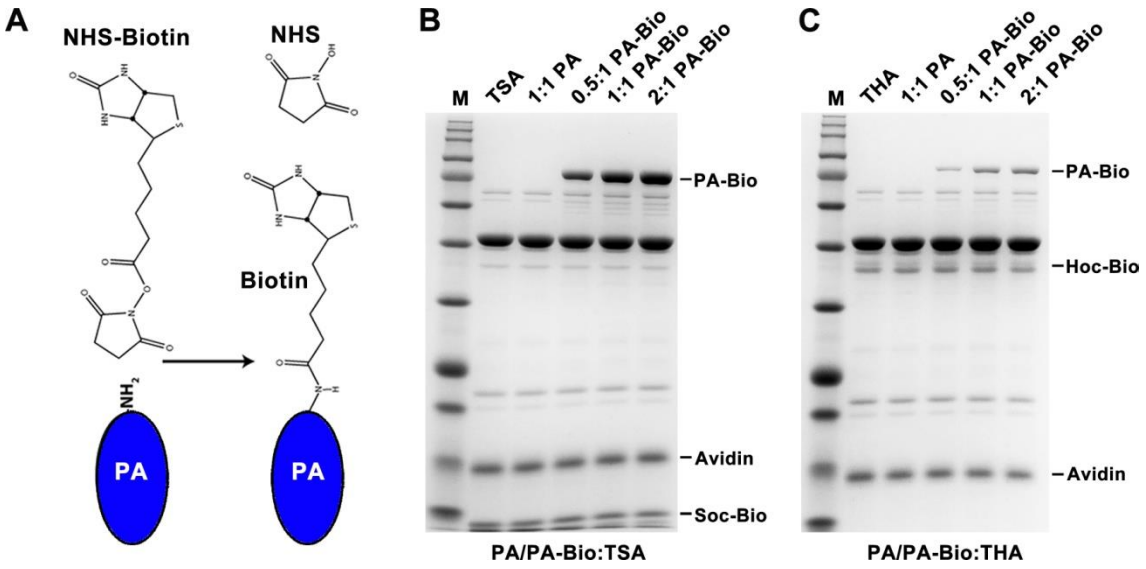

Fig. S2. TSA and THA efficiently bind biotinylated molecules in vitro. (A) Schematic of PA biotinylation. **(B)** and **(C)** Binding of PA and PA-biotin to TSA **(B)** or THA *in vitro* **(C)**. The TSA **(B)** or THA bridges **(C)** were incubated with PA or PA-biotin at increasing ratios (0.5:1 to 2:1). After centrifugation and washing, the samples were analyzed by SDS-PAGE.

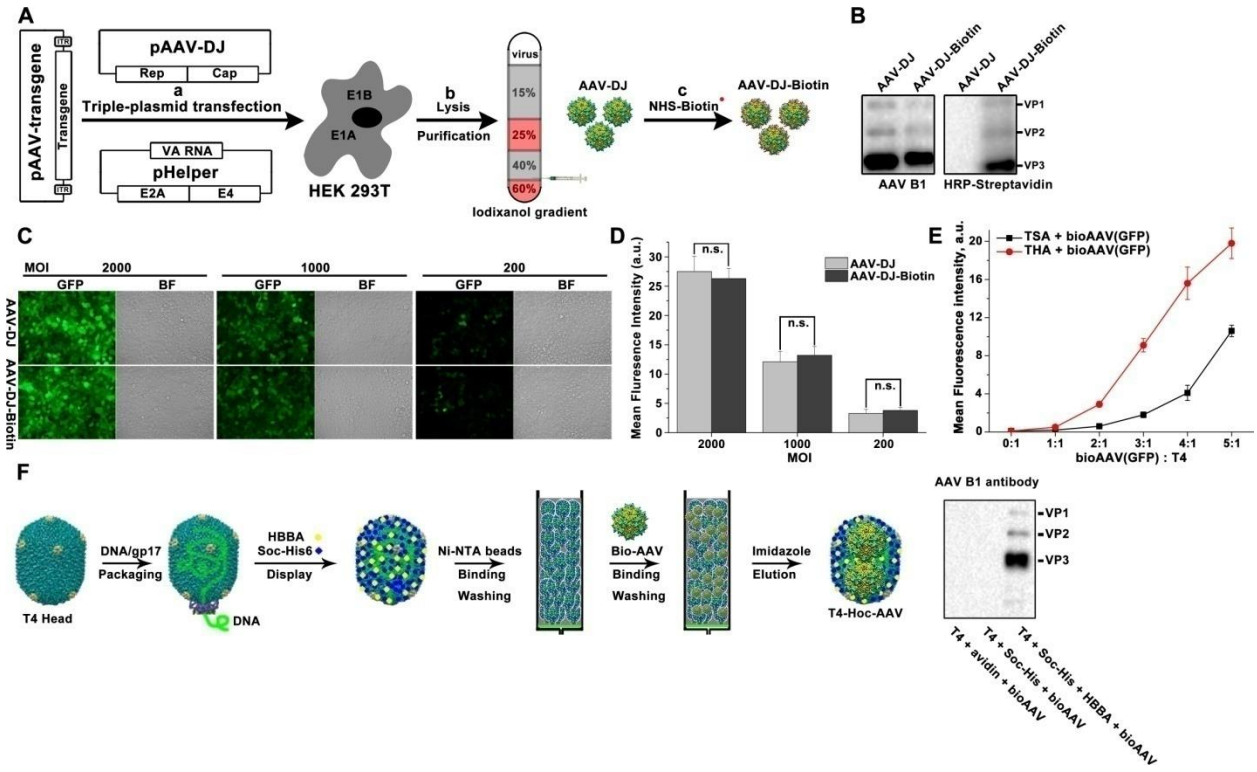

Fig. S3. Recombinant AAV (serotype DJ) efficiently attaches to T4 capsid through biotin-avidin cross-bridges. (A) Schematic drawing of AAV-DJ production, purification, and biotinylation. (a) AAV-DJ production. (b) AAV-DJ purification. (c) AAV-DJ biotinylation. **(B)** AAV-DJ biotinylation was identified by western blot analysis using HRP-streptavidin recognizing biotin conjugated to VP1-VP3. AAV B1 antibody was applied to recognize VP1-VP3 due to their identical C-terminal regions. **(C)** Comparison of the cell transduction efficiencies of unlabeled AAV-DJ and biotinylated AAV-DJ. BF, bright field. **(D)** Quantification of the mean fluorescence intensities of GFP expression in HEK293 cells transduced with unlabeled AAV-DJ(GFP) and biotinylated AAV-DJ(GFP). ns, no significance. Statistical significance was determined using two-tailed Student's *t*-tests. **(E)** Quantification of unbound bioAAV GFP expression in the flow-through fractions. After increasing ratios of bioAAV(GFP) were added to TSA or THA, unbound bioAAV(GFP) in the flow-through fractions was collected and transduced into HEK293 cells. **(F)** Workflow for assembly of the T4-Hoc-AAV vector and identification by western blot analysis using an AAV B1 antibody.

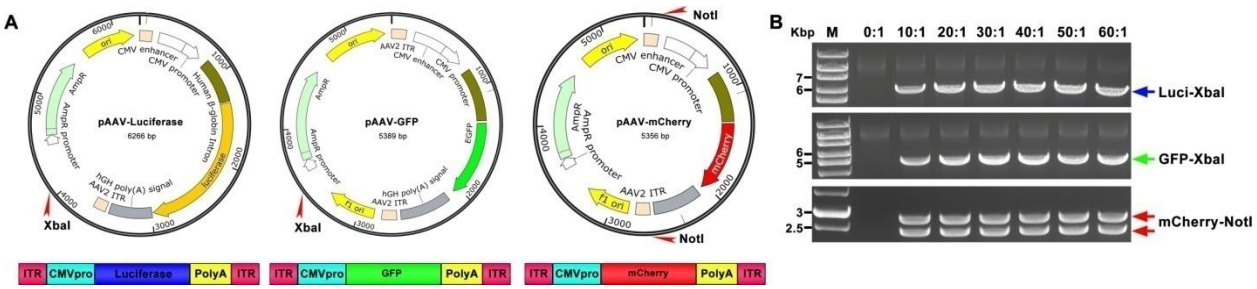

Fig. S4. Characterization of T4 DNA packaging. (A) Schematic representation of DNA vectors and expression cassettes (pAAV-luciferase, pAAV-GFP, and pAAV-mCherry) for packaging. The red arrowheads indicate the endonuclease restriction sites for linearization. **(B)** Determination of the optimal ratio for DNA packaging into the T4 head. The linearized plasmid was incubated with the T4 head at increasing DNA-to-capsid ratios as indicated at the top of the panel.

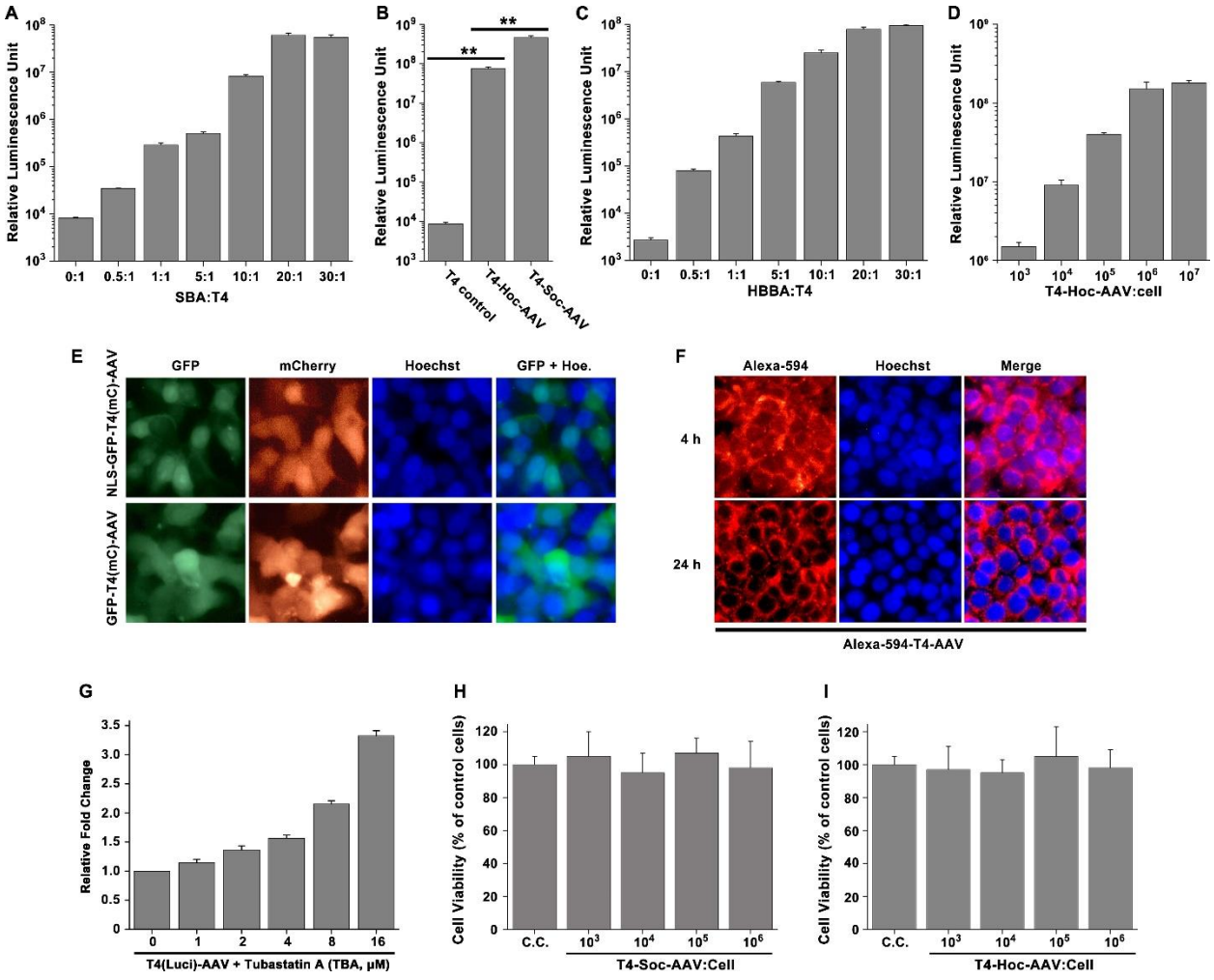

Fig. S5. The T4-AAV vector efficiently delivers packaged DNAs and displayed proteins into mammalian cells without affecting cell viability. (A) Luciferase gene delivery by T4(Luci)-Soc-AAV increases as the SBA binding ratio increases. Higher numbers of displayed SBA molecules indicate a greater chance for bioAAV binding. **(B)** Comparison of luciferase deliveries by T4, T4-Hoc-AAV, and T4-Soc-AAV. **(C)** Increasing the amount of displayed HBBA increased the delivery of luciferase DNA into mammalian cells using T4(Luci)-Hoc-AAV. **(D)** Dose-dependent delivery of the luciferase gene into cells treated with T4(Luci)-Hoc-AAV. **(E)** Internalization and intracellular distribution of the displayed NLS-GFP or GFP proteins and expression of the packaged mCherry DNA in cells treated with NLS-GFP-T4(mCherry)-AAV or GFP-T4(mCherry)-AAV. Cell nuclei were stained with Hoechst. **(F)** Distribution of T4 capsids in

transduced cells. T4 capsid was labeled with Alexa-Fluor-594 and was detected in the cytoplasm at 4 hr and 24 hr post T4-AAV transduction. **(G)** Comparison of luciferase expression in cells transduced with T4(Luci)-AAV with increasing concentrations of Tubastatin A (TBA) normalized to no-TBA treatment. **(H) and (I)** *In vitro* viability of HEK293 cells treated with increasing quantities of T4-Soc-AAV (H) and T4-Hoc-AAV (I). The cell proliferation assay was performed at 48 h post-transduction according to instructions in the CellTiter-Glo Luminescent Cell Viability Assay manual (Promega). Determination of the number of viable cells in culture was based on the quantification of ATP present, which signaled the presence of metabolically active cells. The cell viability of untreated control cells was normalized to 100%. The values represent the mean ± SD of three independent replicates. **p< 0.01. Statistical significance was determined using two-tailed Student's *t*-tests.

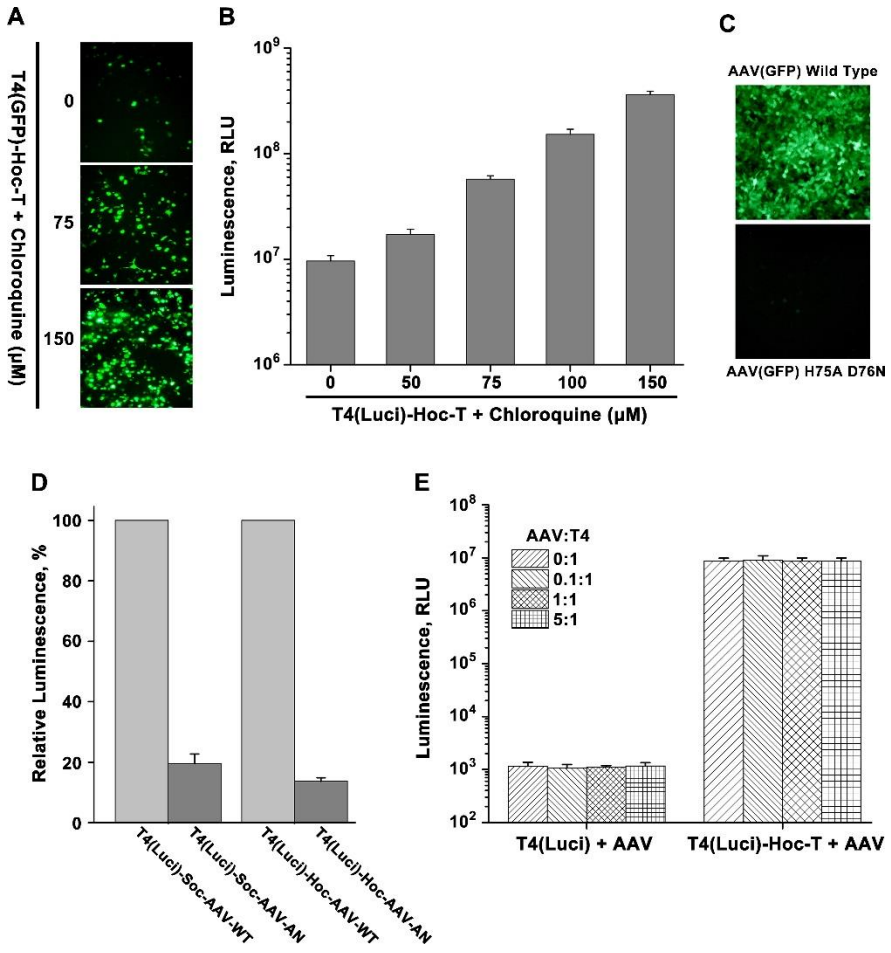

Fig. S6. Endosomal escape is critical for T4-AAV intracellular delivery. (A) and (B) HEK293 Cells were transduced with T4(GFP)-Hoc-TAT (A) or T4(Luci)-Hoc-TAT (B) with increasing concentrations of chloroquine. GFP fluorescence or luciferase assay was observed or performed at 48 h post transduction. **(C)** HEK293 cells were infected with AAV(GFP)-DJ wild-type (WT) and AAV(GFP)-DJ H75A-D76N double mutant (VP1). H75 and D76 are conserved amino acid residues in the catalytic center of Phospholipase A2. GFP expression in cells was assessed at 48 hr. **(D)** Comparison of luciferase deliveries by T4(Luci)-Soc-AAV-WT, T4(Luci)-Soc-AAV-H75A-D76N (AN), T4(Luci)-Hoc-AAV-WT, and T4(Luci)-Hoc-AAV-AN. The luciferase expression of T4(Luci)-Soc-AAV-WT and T4(Luci)-Hoc-AAV-WT was normalized to 100%, respectively. **(E)** Simply mixing T4 or T4-Hoc-T and AAV without conjugation does not improve T4 infection.

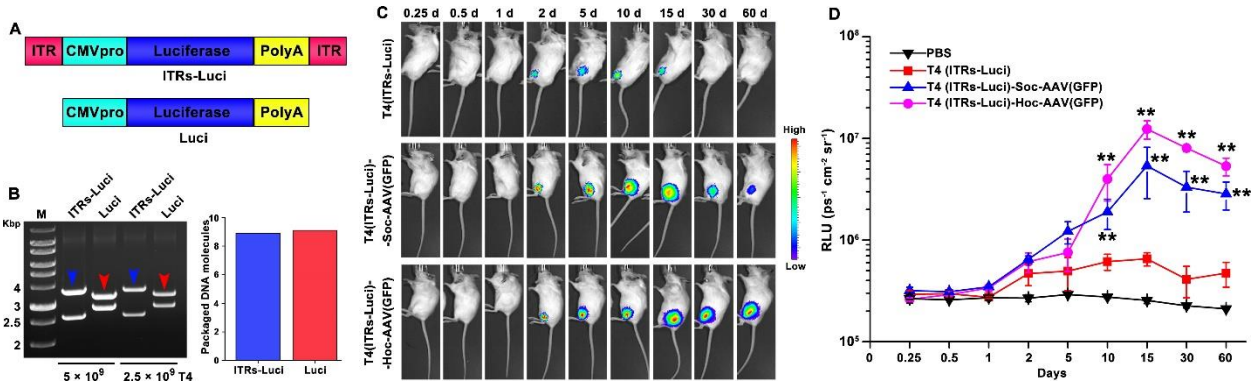

Fig. S7. Representative in vivo bioluminescence images of mice at various time points.

(A) ITRs-luciferase (ITRs-Luci) and Luciferase (Luci) expression cassette. **(B)** Comparison of DNA packaging of ITRs-Luci (blue arrows) and Luci (red arrows) into T4 heads. **(C)** Single doses of 5 × 10^{10} copies of T4 (ITRs-Luci) alone or the T4-AAV vector (conjugated by SBA or HBBA) were injected i.m. into mice, and the mice were live-imaged at various time points post-injection. The bioluminescence scale is indicated to the right of the panel and ranges from the most intense (red) to the least intense (blue) based on radiance intensity. **(D)** The luminescence signal intensities of PBS, T4(ITRs-Luci), T4(ITRs-Luci)-Soc-AAV(GFP), and T4(ITRs-Luci)-Hoc-AAV(GFP) were quantified as photons/second/square centimeter/steradian ($ps^{-1}cm^{-2}sr^{-1}$). The values represent the mean ± SD of three independent replicates. **p< 0.01 compared with T4(ITRs-Luci) alone. Statistical significance was determined using two-tailed Student's *t*-tests.

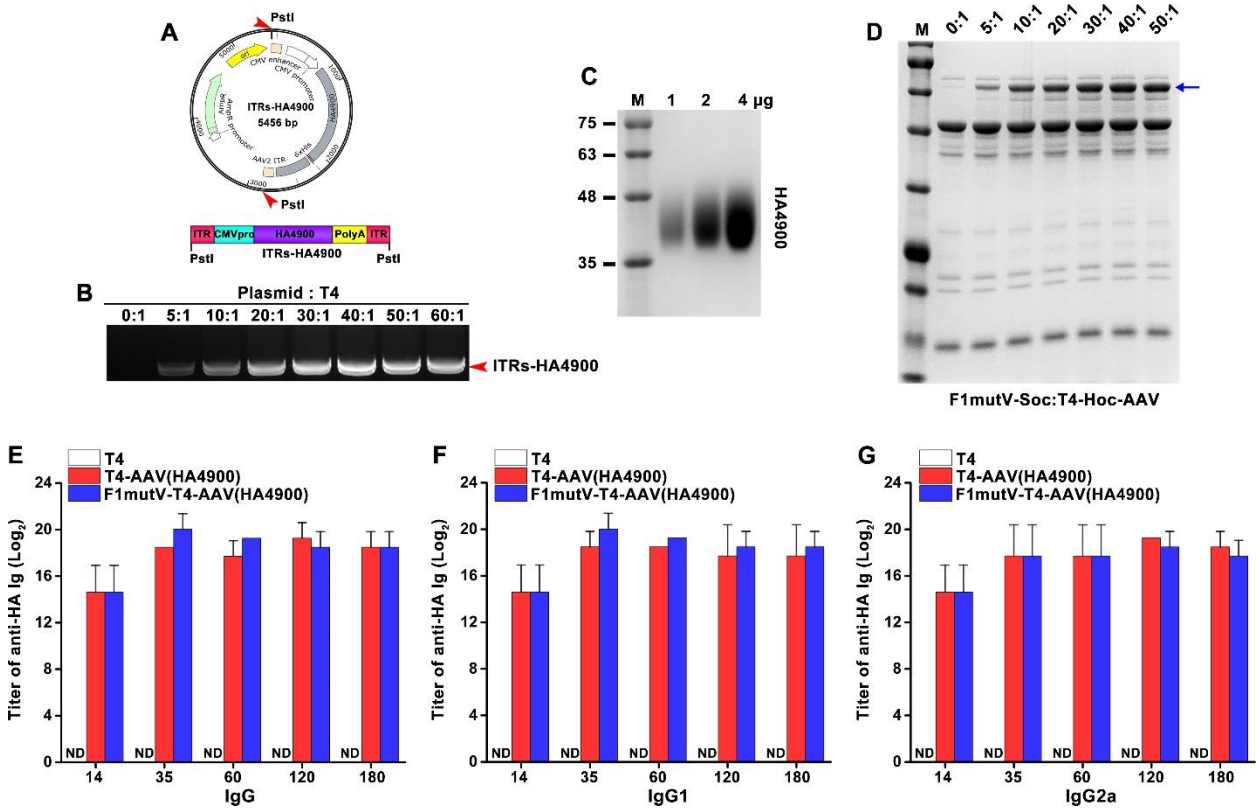

Fig. S8. DNA packaging, protein expression, and antigen delivery by the T4-AAV vector. **(A)** Schematic representation of the DNA vector and expression cassette (pAAV-ITRs-HA4900). The red arrowheads indicate the endonuclease restriction sites for linearization. **(B)** Packaging PstI-linearized HA4900 DNA (red arrowhead) into empty T4 capsids at increasing DNA-to-capsid ratios. **(C)** The SDS-PAGE analysis of produced HA4900 protein. Transduction of T4(HA4900)-AAV particles into HEK293 cells resulted in efficient expression and secretion of the HA4900 antigen into the culture medium. The HA4900 protein was purified from the culture supernatants by metal affinity chromatography and size exclusion chromatography. The peak fractions were pooled, concentrated, and quantified. One, two, and four micrograms HA4900 protein were loaded on SDS-PAGE and stained by Coomassie brilliant blue. **(D)** Display of F1mutV-Soc on the T4 surface of the T4-Hoc-AAV vector. The blue arrow indicates displayed F1mutV-Soc. **(E) to (G)** The titers of anti-HA specific antibody IgG (E), IgG1 (F), and IgG2a (G) were determined by ELISA using sera from mice vaccinated with T4, T4-AAV(HA4900), or

F1mutV-T4-AAV(HA4900) on days 14, 35, 60, 120, and 180. ND, not detected.

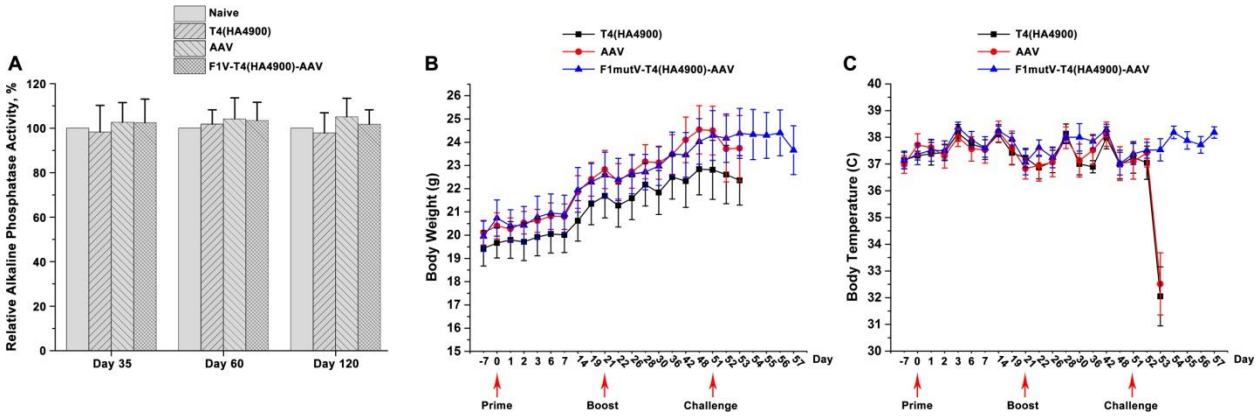

Fig. S9. In vivo toxicity measurement of T4-AAV particles. (A) Alkaline phosphatase activity in mice sera. Mice were immunized with T4(HA4900), AAV, or F1mutV-T4(HA4900)-AAV. The sera were collected on days 35, 60, and 120 and the alkaline phosphatase level was determined using the commercial kit. The alkaline phosphatase activity in naive mice sera was normalized to 100%. **(B) and (C)** Body weight and temperature changes in mice immunized with T4, AAV, or F1mutV-T4-AAV. The mice were monitored daily for body weight and body temperature.

Table S1. Comparison of T4 nanoparticle delivery with other viral delivery platforms.

Vector	Adenovirus	Lentivirus	Adeno-associated virus (AAV)	T4
Genome	dsDNA	ssRNA(+)	ssDNA	dsDNA
Packaging capacity	~7.5 Kbp; Single DNA	~8 Kbp; Single RNA	~4.5 Kbp; Single DNA	Up to ~170 Kbp; Single or multiple DNAs
Protein cargo	No	No	No	Up to ~1025 molecules; Single or multiple proteins
Broad mammalian cell tropism	Yes	Yes	Yes	No natural tropism for mammalian cells
Safety	Presence of Pre-existing Immunity; no integration in host genome; Severe inflammation and immune response	Presence of Pre-existing Immunity; possibility of integration in host genome and likelihood of contamination with replication-competent virus	Presence of Pre-existing Immunity; low possibility of integration in host genome and likelihood of contamination with Adenovirus and wild-type AAV	No pre-existing immunity, unlikely to integrate into the human genome
Production	Mammalian cell derived; expensive and difficult to scale up (yield: 10^9 IFU/ml)	Mammalian cell derived; expensive and difficult to scale up (yield: 10^7-10^8 IFU/ml)	Mammalian cell derived; expensive and difficult to scale up (yield: ~10^{10} genome copies/ml)	Bacterially derived; high yield; can be scaled up relatively easily and inexpensively (yield: 10^{11} empty heads/ml)